

Article

Evaluation of Efficiencies of Locally Available Neutralizing Agents for Passive Treatment of Acid Mine Drainage

Casey Oliver A. Turingan ^{1,*} , Giulio B. Singson ¹, Bernadette T. Melchor ¹, Richard D. Alorro ² , Arnel B. Beltran ¹ and Aileen H. Orbecido ¹

¹ Chemical Engineering Department, De La Salle University, Manila 1004, Philippines; giulio_singson@dlsu.edu.ph (G.B.S.); bernadette_melchor@dlsu.edu.ph (B.T.M.); arnel.beltran@dlsu.edu.ph (A.B.B.); aileen.orbecido@dlsu.edu.ph (A.H.O.)

² Western Australia School of Mines: Minerals, Energy and Chemical Engineering, Curtin University, Kalgoorlie Campus, Kalgoorlie, WA 6430, Australia; richard.alorro@curtin.edu.au

* Correspondence: casey_oliver_turingan@dlsu.edu.ph

Received: 11 August 2020; Accepted: 22 September 2020; Published: 24 September 2020



Abstract: Acid mine drainage (AMD) generated from the mining industry elevates environmental concerns due to the pollution and contamination it causes to bodies of water. Over the years, passive treatment of AMD using alkalinity-generating materials have been widely studied with pH neutralization as its commonly observed mechanism. During the treatment process, heavy metal removal is also promoted by precipitation due to pH change or through adsorption facilitated by the mineral component of the materials. In this study, four materials were used and investigated: (1) a low grade ore (LGO) made up of goethite, calcium oxide, and manganese aluminum oxide (2–3) limestone and concrete aggregates (CA) composed of calcite, and (4) fly ash consisting of quartz, hematite, and magnetite. The performance of each alkalinity-generating agent at varying AMD/media ratios was based on the change in pH, total dissolved solids (TDS), oxidation reduction potential (E_H); and heavy metals (Fe, Ni, and Al) removal and sulfate concentration reduction. Concrete aggregate displayed the most significant effect in treating AMD after raising the pH to 12.42 and removing 99% Fe, 99% Ni, 96% Al, and 57% sulfates. Afterwards, the efficiency of CA at various particle sizes were evaluated over 1 h. The smallest range at 2.00–3.35mm was observed to be most effective after 60 min, raising the pH to 6.78 and reducing 94% Fe, 78% Ni, and 92% Al, but only 28% sulfates. Larger particles of CA were able to remove higher amounts of sulfate up to 57%, similar to the jar test. Overall, CA is an effective treatment media for neutralization; however, its performance can be complemented by a second media for heavy metal and sulfate removal.

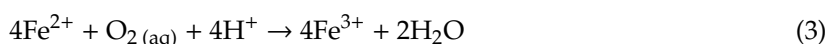
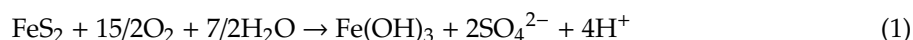
Keywords: iron hydroxide; iron oxyhydroxide; acid mine drainage; nickel ore; fly ash; concrete aggregate; calcite; goethite; hematite; magnetite; quartz

1. Introduction

Acid mine drainage (AMD) is known as one of the worst environmental problems worldwide related to mining, mineral processing operations, and other large-scale excavations [1,2]. It is characterized by low pH and high concentrations of sulfate, heavy metals, and other toxic elements, which cause negative effects to the surrounding areas [3,4]. In the United States, there is an estimated 20,000 to 50,000 mines capable of impacting up to 10,000 miles of water bodies, since 90% of the mines are abandoned [5]. Other countries with a large number of mines include Australia (52,534), Canada (10,139), South Africa (>6000), Japan (5487), China (>5000), the UK (>2000), and South Korea (1692) [6]. In the Philippines, the mining industry has significantly contributed to the economy with

an estimated \$840 billion worth of mineral wealth that had not been extracted as of 2012 [7]. In 2019, the industry contributed 0.6% to GDP and 6% of the total exports, which amounted to approximately \$2 billion and \$4.3 billion, respectively [8]. However, generation of AMD from several AMD-generating mine sites has posed a detrimental effect on the environment [4].

One of the main and most common minerals responsible for AMD is pyrite (FeS₂) [9]. It is typically found in sediments, ore deposits, mineralized veins, hydrothermally altered rocks, and soils [3,10]. As mining activities expose pyrite and other sulfide-bearing ores to oxygen and water, AMD production accelerates [11]. Pyrite oxidation is facilitated by various reactions that occur in different situations as shown in Equations (1)–(6) [9,12].



Equation (1) describes pyrite oxidation when exposed to oxygen and excess water at a neutral pH. On the other hand, Equation (2) utilizes Fe³⁺ as the oxidizing agent with excess water and proceeds at a faster rate compared to that of Equation (1) [13]. In this case, Fe³⁺ is generated by Equation (3) or through iron-oxidizing bacteria [12]. Equation (4) shows the electrochemical reaction which occurs in aqueous systems. Dissolved oxygen and Fe³⁺ are reduced in their respective cathodic sites through the electrons (Equations (5) and (6)) transferred from the anodic sites of the pyrite crystal until its dissociation [14]. Equation (7) represents the complete oxidation of pyrite in low water content. This reaction is accompanied by the odd formation of goethite (α-FeOOH) or schwertmannite (Fe₈O₈(OH)₆·nH₂O) [15]. As the oxidation process occurs, acidic water interacts with rocks containing various minerals and dissolves toxic metals along the way. Fe, Al, sulfate, and bicarbonate are the most common ions dissolved in AMD [2]. Moreover, pyrite alone is known to be incorporated with As, Pb, Cu, Zn, Se, and B, depending on its source [3].

The pollution caused by AMD in bodies of water poses a serious threat to surrounding flora and fauna [4]. Thus, proper treatment of acid mine drainage is necessary during and after operations. Generally, not all mine sites have the same AMD potential, and thus different active and passive treatments are employed in treating produced AMD from various mine sites [11,16,17]. Active treatments include using alkaline metals to precipitate metals, adsorption, ion exchange, and membrane technology, among others [9]. These methods are typically used to treat AMD with very high levels of acidity while being capable of adjusting to the varying geochemical properties. However, active treatment is limited by its cost and sludge generation, making it unsustainable in the long run [6]. In comparison, passive treatments are considered to be more cost-effective to use in a closed and abandoned mine site due to the stable chemistry at these mine sites as well as the accessible land for remediation systems [16,18]. As a result of several closed and abandoned mine sites in the Philippines, passive treatment is employed in this study [19].

In the passive treatment of AMD, some of the materials used that generate alkalinity are limestone (CaCO₃), lime (CaO), hydrated lime (Ca(OH)₂), pebble quicklime (CaO), periclase (MgO), magnesite (MgCO₃), brucite (Mg(OH)₂), dolomite (MgCO₃·CaCO₃), fly ash, soda ash (Na₂CO₃), caustic soda (NaOH), and ammonia (NH₃) [16,20,21]. AMD is treated through pH neutralization as the materials generate alkalinity through the reaction of oxide minerals present. Limestone is the main material in some passive treatment systems such as open limestone channels (OLCs), open limestone

drains (OLDs), and limestone leaching beds (LLBs) [22–24]. However, a major drawback encountered in these systems is the armoring with hydroxides when heavy metal concentrations, specifically Fe, are too high [25]. In addition, these systems are unable to treat AMD with pH < 2 and flows greater than 50 L/s. Moreover, effluents would only reach up to pH 8, rendering the treatment ineffective against some heavy metals with higher solubilities [6]. In addition, waste by-products were also used as an alkalinity-generating material. These waste by-products are eggshell waste [26], wood ash [27], phosphatic waste rock [28], and concrete aggregate [29]. Another material used in recent studies was serpentinite ((Mg,Fe,Ni,Al,Zn,Mn)_{2–3}(Si,Al,Fe)₂O₅(OH)₄) found in mining waste rock that belongs to the serpentine group of minerals considered as alkaline-rich [30,31]. After a series of batch experiments, serpentinite was able to raise the pH of the AMD to 4.5, 5.5, and 6.5–8.5 for the first, second, and third series of experiments, respectively [32]. In terms of metal removal, the mineral was able to remove 99.95–100% Fe, 85.7–98.9% Al, and 27.3–28.8% SO₄ from the synthetic acid mine drainage.

In the Philippines, nickel mines are ubiquitous and account for 29 out of 104 operational mines in the country [8]. However, only those containing >1.4% Ni are eligible for exportation, with the remaining material considered as low-grade ore (LGO). This is combined with deposits that have relatively high purity to meet the standard; otherwise, the LGO will be stockpiled in mine sites. The stock would then act as a source of pollution when its runoff flows to nearby streams. In order to repurpose LGO, it was characterized and its potential to treat AMD was evaluated. Goethite was identified as a major component. Moreover, LGO was able to remove >99% Fe and Al, 94% Ni, and 93% of sulfate despite only raising pH from 2.21 to 5.36 [33]. This shows the potential of LGO to complement an alkaline-generating material in treating AMD to make up permeable reactive barriers. Permeable reactive barriers are an example of an in situ passive treatment wherein the contaminants are immobilized via adsorption, precipitation process and ion exchange. Some examples of these are iron oxyhydroxides (FeOOH), iron oxides (Fe_xO_y), and carbonates (CO₃²⁻). Iron oxyhydroxides naturally occurs as the following minerals: α-FeOOH (goethite), β-FeOOH (akageneite), γ-FeOOH (lepidocrocite), and δ-FeOOH (feroxyhyte). Among the polymorphs of FeOOH, its most common form occurs as goethite and lepidocrocite. Past studies made use of these minerals in the adsorption of cadmium (Cd), copper (Cu), zinc (Zn), lead (Pb), selenium (Se), and chromate (CrO₄²⁻) [34–36].

Even though limestone has been widely studied, its limitations generated from previous studies due to its low solubility above pH 7 and armoring have led the researchers of this study to look for alternative alkalinity-generating materials [2]. Concrete aggregate, fly ash, and low-grade nickel ore are waste materials in abundant supply locally and are considered to be excellent alternatives. Concrete aggregate makes up as much as 50% of municipal solid waste while 1.4 MMT of fly ash is generated annually [37,38]. In addition, these materials have varying composition compared to those used in previous studies, and thus, performance in AMD treatment would also differ. Hence, this study is conducted to evaluate the efficiencies of low-grade nickel ore, fly ash, and concrete aggregate in comparison with limestone in passive treatment of AMD. The treatment efficiencies were evaluated in terms of the geochemical properties and the heavy metal and sulfate concentration of the treated AMD.

2. Materials and Methods

2.1. Materials and Reagents

Low-grade nickel ore (LGO), limestone, fly ash, and concrete aggregates were the four locally available neutralizing agents compared based on their efficiencies in treating acid mine drainage (AMD). LGO and limestone were both collected from a mine site in Mindanao, Philippines. Fly ash was obtained from a coal-fired power plant situated in Bataan, Philippines; while concrete aggregates were collected from a local construction site in Manila, Philippines. Concrete aggregate and limestone were crushed and sieved through a mesh size 20 (<841 μm) to obtain their powder form. LGO and fly ash were left as they were since particle size analysis was not possible for these during the study.

2.2. Synthetic Acid Mine Drainage Preparation

The treatment efficiencies of the neutralizing agents were evaluated with a synthetic solution of acid mine drainage (AMD) based on Bernier (2005) [32]. The synthetic AMD was prepared with analytical grade reagents diluted to 7 L of distilled water, as shown in Table 1. Then 1.5 M sulfuric acid was carefully added dropwise to adjust the acidity of the synthetic solution. The geochemical properties of the synthetic solution, including the metals (Fe, Ni, and Al) and sulfates content are immediately measured, which are summarized in Table 2.

Table 1. Reagents needed for synthetic acid mine drainage (AMD) preparation.

Reagents	Mass (g)
FeSO ₄ ·7H ₂ O	65.46
Al ₂ (SO ₄) ₃ ·18H ₂ O	17.28
NiSO ₄ ·6H ₂ O	9.39
CuSO ₄ ·5H ₂ O	1.4
MnSO ₄ ·H ₂ O	1.4
MgSO ₄ ·7H ₂ O	1.4
1.5 M H ₂ SO ₄	60 mL

Table 2. Geochemical properties and metal content of synthetic AMD.

Parameter	Measurement
pH	2.44
Oxidation-Reduction Potential (E _H)	453.6 mV
Conductivity	6.98 mS/cm
Total Dissolved Solids (TDS)	3420.5 ppm
Fe	1647.48 ppm
Ni	302.49 ppm
Al	690 ppm
Sulfates	30,350 ppm

2.3. Characterization of Neutralizing Agents

The four types of neutralizing agents were analyzed for their whole-rock chemistry and mineralogy. The chemistry of the materials was determined using X-ray Fluorescence (Horiba Scientific XGT-7200 X-ray Analytical Microscope, HORIBA Ltd., Kyoto, Japan). The samples were dried to 105 °C to remove the free moisture content before undergoing actual XRF procedures. Meanwhile, X-ray Diffraction was employed to analyze their mineralogy using Shimadzu LabX XRD-6100 X-ray Diffractometer (Shimadzu Scientific Instruments, Columbia, MD, USA) at step size = 0.02° over a 5–60° 2θ range. Furthermore, limestone and concrete aggregates underwent mechanical crushing and sieving in order to obtain fine powder particles (<0.841 mm) similar to the other two samples of neutralizing agents (LGO and fly ash).

2.4. Jar Test Using Different Alkaline-Generating Materials

For the first batch of experiment, an overhead stirrer (Lovibond Floc Tester, Tintometer Inc., Dortmund, Germany) was employed to evaluate the efficiency of each neutralizing agents in treating synthetic AMD with various AMD/Media ratios of 0.75, 1.0, 1.5, and 2.0 mL/g. Constant mixing at 180 rpm was done for 1 h. Afterwards, the mixtures settled for 30 min before collecting 50 mL of the supernatant for analysis.

2.5. Batch Test Using Various Particle Sizes

In order to determine the effect of varying particle sizes, concrete aggregate, the most efficient neutralizing agent from the jar test, was utilized. The material underwent crushing and mechanical sieving to obtain particle sizes of 4.75 mm, 3.35 mm, and 2.00 mm. Similarly, the AMD/Media ratio of 0.75 mL/g wherein the four neutralizing agents performed best was used in this set of runs. In each run, enough AMD is poured into the reactor containing concrete aggregate to achieve the desired AMD/media ratio. Samples are obtained at specific time intervals through a spout located at the bottom of the reactor (Figure 1). Analysis of geochemical properties, heavy metals, and sulfates content were done for all treated samples from both batch experiments. Benchtop meters were used to measure geochemical properties of the treated samples, specifically: pH, reduction-oxidation potential (E_H), conductivity, and total dissolved solids (TDS). On the other hand, heavy metals and sulfate content were analyzed through atomic absorption spectrometry (AAS) (Shimadzu AA-6300, Shimadzu Scientific Instruments, Columbia, MD, USA) with the following detection limits: Fe, 0.06–15 ppm; Ni, 0.1–20 ppm; Al, minimum DL = 0.01 ppm; sulfates, minimum DL = 1 ppm.

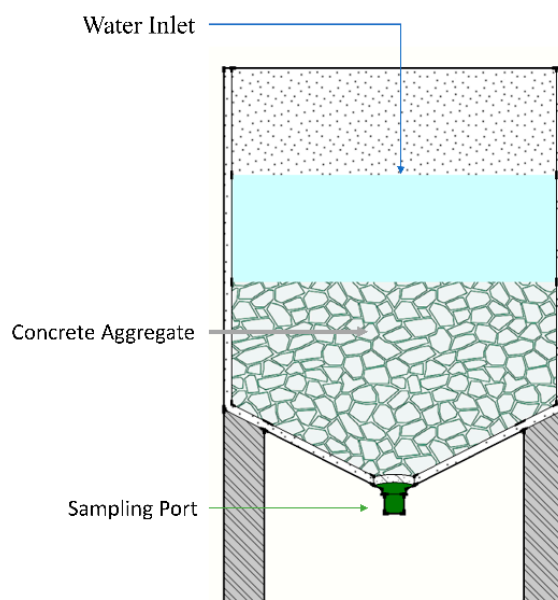


Figure 1. Schematic diagram of the batch test reactor.

2.6. Geochemical Modeling

Geochemical models were developed to complement the experimental results and allow further insight into the processes during the treatment of AMD. PHREEQC Interactive v.3.6.2 (USGS, Reston, VA, USA) [39] was used to calculate the saturation indices of potential precipitates using the THERMOCHEM database from the BGRM Institute, and the data obtained from AAS analysis. Ca and HCO_3^- were counted in the effluent solution to consider the dissolution of calcite from limestone and concrete aggregates. On the other hand, Ca was included for the fly ash-treated effluent. These ions were incorporated to show the precipitates that may form when AMD is treated with these materials.

3. Results

3.1. Whole Rock Chemistry

The whole rock chemistry of the materials in terms of their oxide composition is presented in Table 3. Furthermore, oxide composition of the concrete aggregate provided was taken from literature [40–42] since no actual analysis was available.

Table 3. Percentage of oxide composition of neutralizing agents.

Element	Material			
	LGO	Limestone	Fly Ash	Concrete Aggregate [40–42]
Al ₂ O ₃	4.19	0.93	8.55	4.71 ± 1.50
CaO	4.56	85.66	16.04	58.57 ± 11.68
Fe ₂ O ₃	54.07	7.59	44.63	4.11 ± 1.88
MgO	7.96	0.02	n/a	1.38 ± 1.01
SiO ₂	23.87	1.78	24.65	26.63 ± 9.75
NiO	2.13	0.76	n/a	n/a
Others	3.22	3.26	6.13	4.03 ± 1.87

n/a = metal oxide was not included in the analysis.

Table 3 shows that LGO is mainly comprised of iron oxide in the form of Fe₂O₃ (54.07%), followed by silicon dioxide (23.87%). Other oxides present are aluminum (4.19%), calcium (4.56%), magnesium (7.96%), and nickel (2.13%). Basic oxides in the form of CaO, MgO, and NiO are only less than 10% in total which suggests that LGO would raise the pH but not to a neutral pH. Additionally, SiO₂, which makes up for 23.87% of the sample is considered a very weak acidic oxide and would mean that it could be factor in decreasing the pH even for a little amount.

The limestone used consisted of 85.66% CaO with less than 10% other metal oxides. CaO, MgO, and NiO are among the basic oxides that exist in limestone and would suggest that it would be able to successfully neutralize the AMD. On the other hand, fly ash was mainly composed of Fe₂O₃ (44.63%) and SiO₂ (24.65%), similar to LGO. Although fly ash is comparable to LGO, its performance can be varied as its CaO content is greater. Its SiO₂ content, however, may also limit its capability in neutralizing the solution.

Lastly, numerous studies show that concrete aggregate [40–42] has CaO and SiO₂ as its main components. The presence of CaO in this material suggests that it has the potential to increase pH of acidic solutions, in this case, AMD.

3.2. Mineralogy

Figure 2 shows the presence of goethite in LGO along with calcium oxide and manganese aluminum oxide. Goethite is a form of an iron oxyhydroxide, and in their poorly crystalline form holds higher surface area and smaller site density [43,44]. The presence of higher surface area and smaller site density of iron oxyhydroxides makes its sorption capabilities more extensive [45].

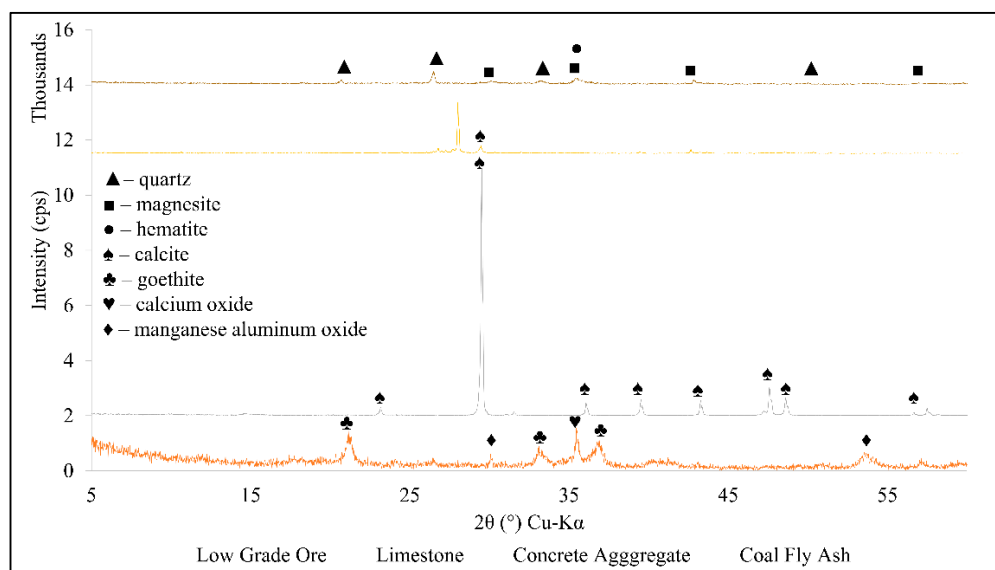


Figure 2. X-ray diffraction of raw low-grade ore, limestone, concrete aggregate, and coal fly ash.

Limestone, on the other hand, is mostly composed of the mineral calcite (CaCO_3), which is also the same with the XRD results from past studies [46,47]. Whereas results for fly ash show that quartz, magnetite, and hematite are the minerals present in the sample. Lastly, concrete aggregate had similar result with limestone having calcite on its peaks.

3.3. Jar Test Using Various Neutralizing Agents

The geochemical properties of AMD treated using the four neutralizing agents are shown in Figures 3–6. The highest pH recorded was 11.53 using concrete aggregates at 0.75 mL/g AMD/Media ratio. Furthermore, all four materials had similar trends wherein the highest pH attained was observed at the lowest ratio (0.75 mL/g). Among the four, LGO appeared to have the minimum neutralizing capability as it only raised the pH to 4.66; while limestone was able to raise the pH of the solution to a value of 6.62 whereas fly ash was capable of neutralizing the solution and raising the pH up to 9.34. Finally, the trend for the change in pH, expected to be based on their alkaline component, CaO, was not followed.

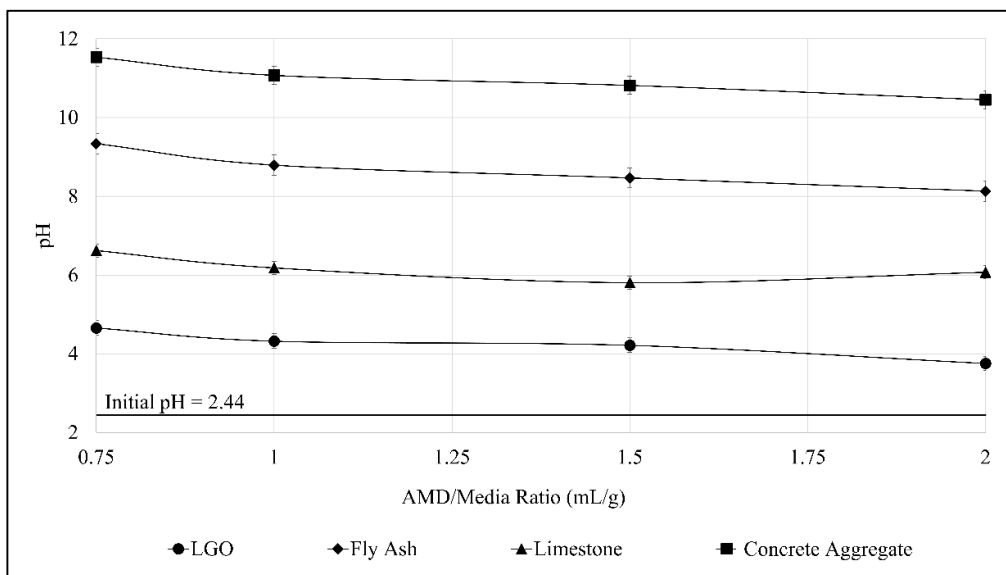


Figure 3. Effect of AMD/Media ratio on pH after 1-h mixing.

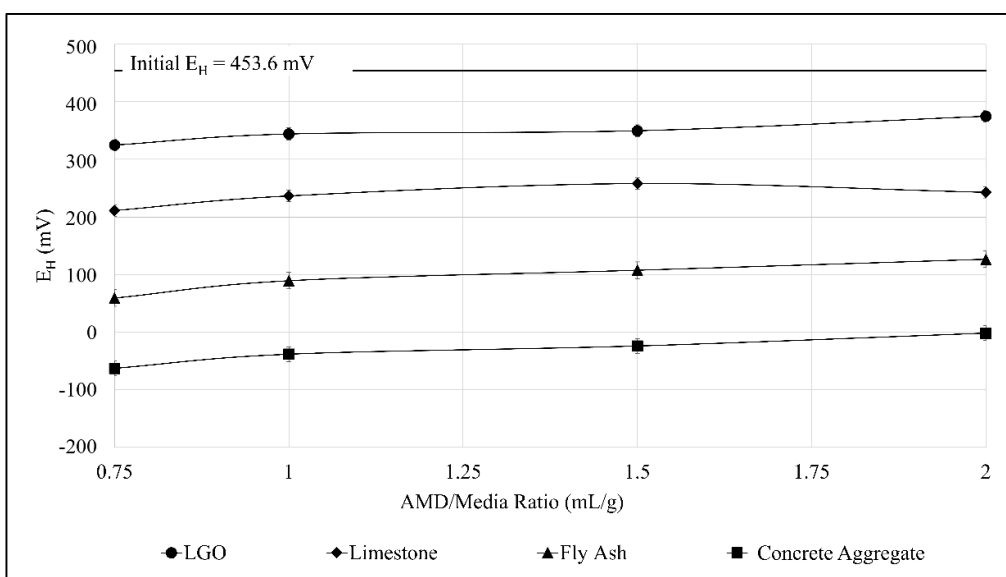


Figure 4. Effect of AMD/Media ratio on E_H after 1-h mixing.

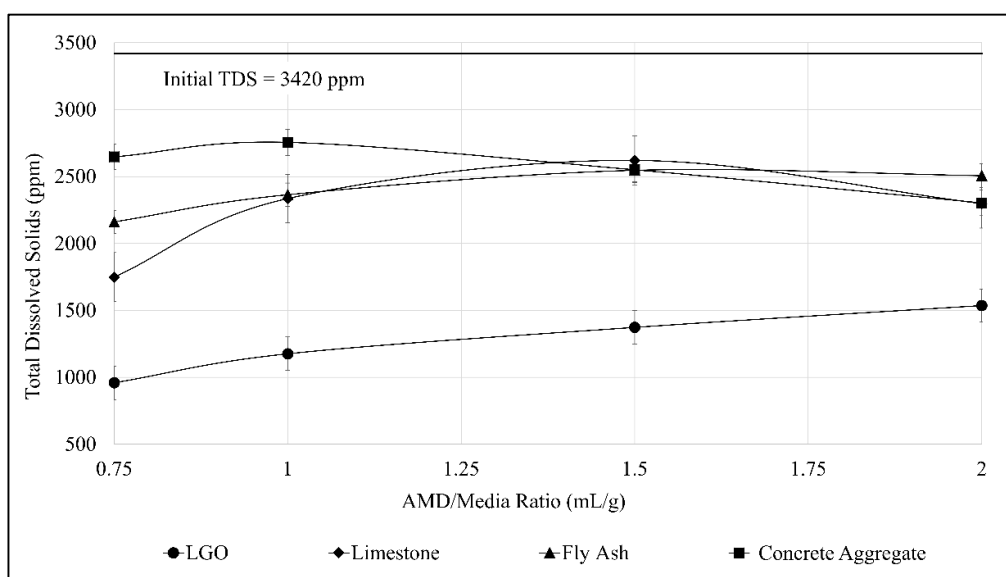


Figure 5. Effect of AMD/Media ratio on total dissolved solids (TDS) after 1-h mixing.

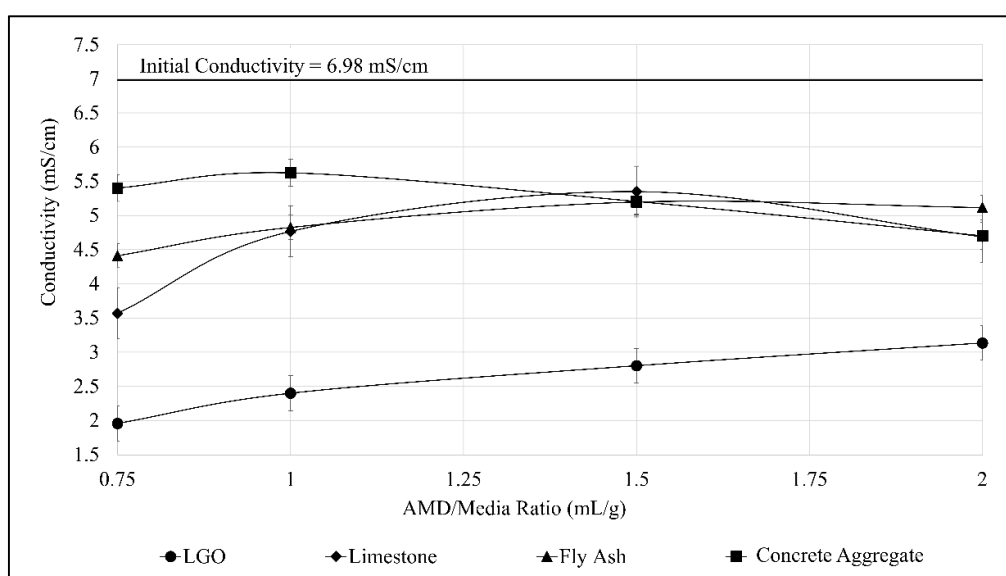


Figure 6. Effect of AMD/Media ratio on conductivity after 1-h mixing.

The initial E_H reading of the synthetic solution was 254 mV. After conducting jar test, the AMD treated with concrete aggregate and fly ash caused the redox potential of the solution to be negative. The AMD treated with LGO still had a high redox potential close to the initial value since the solution was still essentially acidic as it was not able to get neutralized significantly.

The AMD treated using a ratio of 0.75 mL/g had the lowest value of total dissolved solids (TDS) and conductivity for all neutralizing agents. After jar test, LGO-treated AMD at 0.75 mL/g ratio had the lowest TDS and conductivity suggesting that low-grade ore was able to remove the most amount of heavy metals from the synthetic solution. Meanwhile, TDS and conductivity results from the solution treated by limestone had a significant increase when ratio of 1.0 and 1.5 were used, then had a decrease when the ratio of 2.0 was employed. Heavy metal ions were removed through adsorption onto goethite present in LGO while precipitation is the main suspect in the removal of heavy metal ions in the other three materials which resulted to a more alkaline effluent [33,40,48]. In relation to its pH results, ratio 1.5 for limestone also had the lowest pH attained which could suggest that heavy metals in AMD were not able to precipitate as much at that pH level as compared to the other ratios.

The comparison for the metals (Fe, Ni, and Al) and sulfate concentrations of the initial and treated synthetic AMD is shown in Figure 7. The trend of removal was expected wherein the lowest AMD/Media ratio corresponds to the highest removal of metals and sulfates for each material used. For iron, the removal was fairly consistent at 99% at ratio of 0.75 up to 1.5 mL/g for LGO and all ratios using fly ash and concrete aggregate. Meanwhile for nickel, removal was only at most 80% using LGO and 70% for limestone; but it attained almost complete removal when fly ash and concrete aggregate were used with any of the ratios employed. Aluminum also reached complete removal as high as 98% using LGO at 0.75 mL/g, while only achieving 82% at 2.0 mL/g, which was the highest removal for aluminum among the four materials. Nevertheless, out of the four metals and sulfates, iron was removed most efficiently wherein complete removal was almost achieved at >99% for all neutralizing agents.

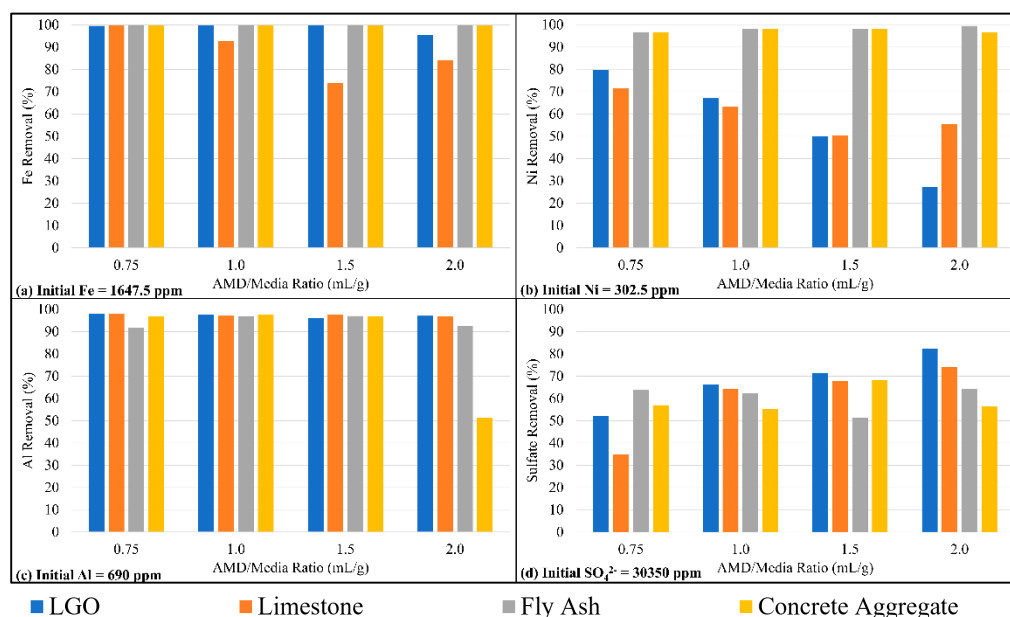


Figure 7. Effect of AMD/Media ratio on the removal of (a) iron; (b) nickel; (c) aluminum; and (d) sulfates.

3.4. Effect of Particle Size on AMD Treatment

After the treatment of AMD, the highest pH measured was 6.78 at the 60-min interval of 3.35 mm–2.00 mm size range; whereas pH obtained upon using 4.75 mm–3.35 mm was at 6.42; and pH 6.16 was obtained using 4.75 mm (Figure 8a). The results do not reflect a similar behavior of the concrete aggregate material as seen in the previous experiment. This may be due to the slow dissolution rate of Ca-based compounds which is slower compared to that of other chemicals, and thus there is a need for mechanical mixing to increase its neutralizing capacity [49].

In comparison with the result obtained from using concrete aggregate in the jar test which resulted to 99.64% removal for Fe and 99.69% removal for Ni, percent removals acquired for the batch experiment (Figure 9) have significant difference which may be accounted to the improved optimal surface exposure provided by the constant mechanical mixing, as compared to the undisturbed contact between the concrete aggregate and AMD without mechanical mixing. Additionally, only little amount of Ni was removed from the AMD solution after 1-h treatment. Again, the smallest particle size was still able to remove more metals than compared to the other two sizes as it had the largest total surface area reacting with the synthetic solution.

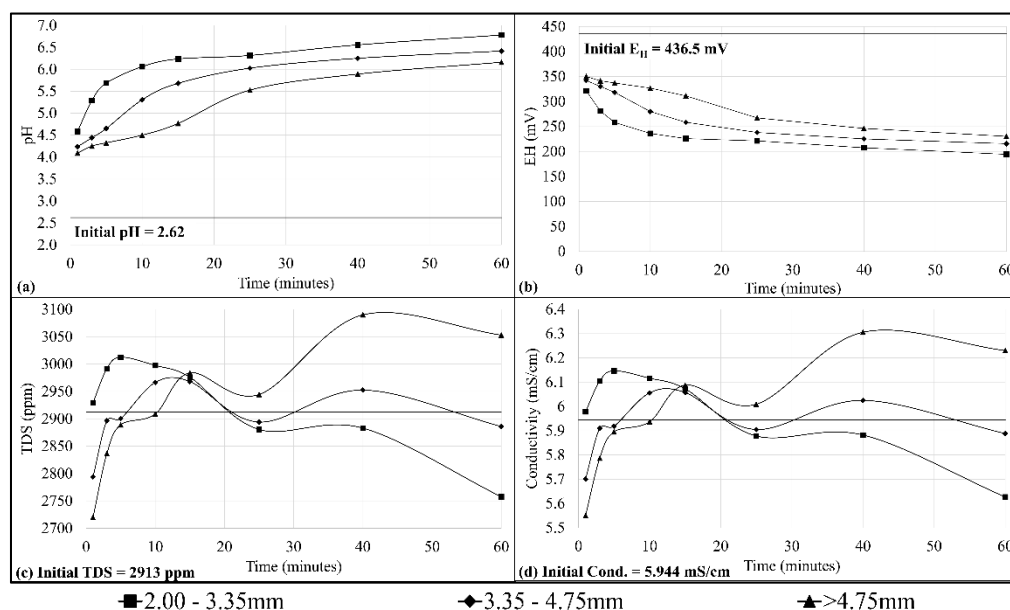


Figure 8. Effect of particle size on (a) pH; (b) E_H ; (c) TDS; and (d) conductivity after 1-h contact.

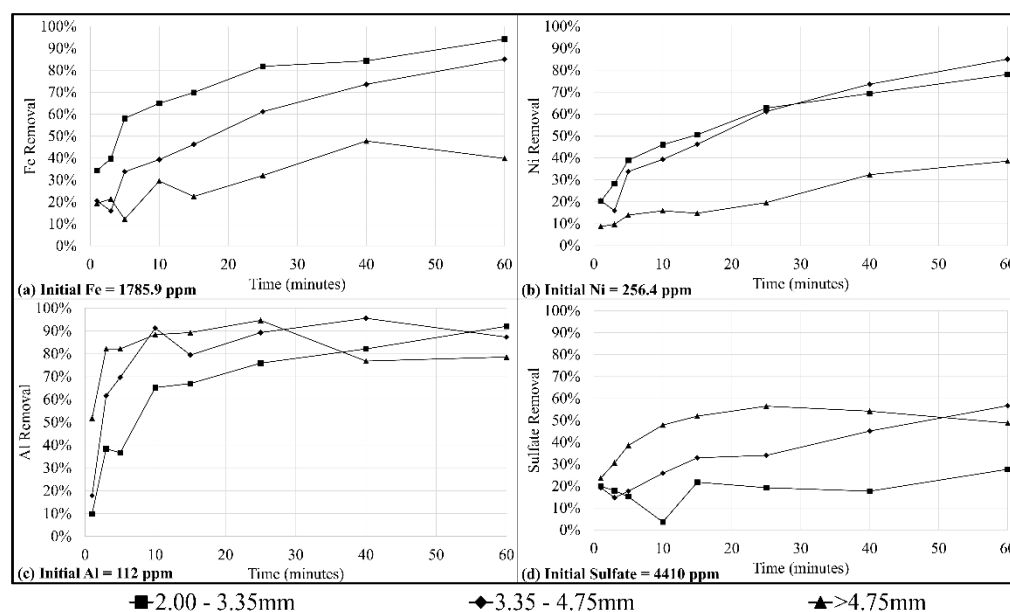


Figure 9. Effect of particle size on the removal of (a) iron; (b) nickel; (c) aluminum; and (d) sulfates.

4. Discussion

4.1. Comparison of the Treatment Efficiencies of Various Neutralizing Agents

Low grade ore (LGO) caused a slight change in pH of synthetic AMD from 2.44 to 4.46 at the 0.75 ratio. However, this material caused the largest decrease in total dissolved solids and conductivity, suggesting that it was able to remove the largest amount of metals and sulfates from the solution. Its performance can be attributed to the capabilities of goethite to adsorb metals such as nickel, copper, manganese, and aluminum [50], including sulfates [51]. Such capabilities of goethite hold true as it is often poorly crystalline and rich in impurities that makes it have high specific surface area with good surface activity. Furthermore, the material's surface area and site density are important factors for determining its capabilities as a good adsorbent [50]. Aluminum may not only be adsorbed onto the surface of goethite but also substitute some of the Fe on the surface by as much as 33 mol% to form

Al-FeOOH [52]. This compound has shown a higher adsorption rate of Ni in comparison to goethite through inner-sphere surface complexation [53]. PHREEQC suggests that some precipitates formed, such as anhydrite (CaSO_4), gypsum ($\text{CaSO}_4 \cdot 2\text{H}_2\text{O}$), bassanite ($\text{CaSO}_4 \cdot 0.5\text{H}_2\text{O}$), diaspore ($\text{AlO}(\text{OH})$), boehmite ($\text{AlO}(\text{OH})$), and gibbsite ($\text{Al}(\text{OH})_3$), in decreasing saturation indices (SIs). During their formation, Ni and sulfate ions co-precipitate with the aluminum hydroxides, resulting in a higher sulfate removal at a higher ratio when using LGO as treatment media [54].

Limestone was not able to successfully neutralize the synthetic AMD, thus revealing its limitation in neutralization that may be due to its low solubility and armoring. The latter occurs after the initial neutralization process when Fe precipitates on the surface of the limestone, slowing down the rate of its dissolution [21]. Based on geochemical modeling, these are magnetite (Fe_2O_3), goethite (FeOOH), lepidocrocite (FeOOH), and ferrihydrite ($\text{Fe}(\text{OH})_3$), and siderite (FeCO_3). Other precipitates were diaspore, boehmite, gibbsite, gypsum, and bassanite. Nonetheless, results obtained from treating AMD with limestone were expected to be and were indeed consistent in comparison to past studies, as it has a neutralizing capability ranging from pH 6.00 to 7.5 [55]. Nickel is still quite soluble at this range, suggesting that its removal may have been mainly due to co-precipitation and cation sorption on the surface of the Fe and Al precipitates [56].

Fly ash performed better in increasing the pH of AMD despite containing 16.04% CaO only. This shows that the CaO component in fly ash is more readily dissolved relative to that of limestone. Other studies have observed a similar change in pH and attributed it to the dissolution of the fly ash [43,57,58]. At the pH level reached using this material, PHREEQC suggested the precipitation of the following: dolomite ($\text{CaMg}(\text{CO}_3)_2$), hydrotalcite ($\text{Mg}_3\text{Al}_2(\text{OH})_6 \cdot 3\text{H}_2\text{O}$), magnesite, diaspore, boehmite, gibbsite, NiCO_3 , nesquehonite ($\text{MgCO}_3 \cdot 3\text{H}_2\text{O}$), lansfordite ($\text{MgCO}_3 \cdot 5\text{H}_2\text{O}$), artinite ($\text{Mg}_2(\text{OH})_2(\text{CO}_3) \cdot 3\text{H}_2\text{O}$), spinel (MgAl_2O_4), gypsum, and anhydrite. Concrete aggregates had the highest effluent pH = 11.75. This allowed the precipitation of Ni compounds, specifically NiCO_3 and $\text{Ni}(\text{OH})_2$. PHREEQC also showed the formation of ettringite ($\text{Ca}_6\text{Al}_2(\text{SO}_4)_3(\text{OH})_{12} \cdot 26\text{H}_2\text{O}$), magnetite, goethite, lepidocrocite, ferrihydrite, diaspore, boehmite, gibbsite, gypsum, and anhydrite. Iron compounds had the highest SIs, followed by those containing nickel, then aluminum, and sulfates.

Overall, oxyhydroxides had relatively high SIs followed by hydroxides, gibbsite ($\text{Al}(\text{OH})_3$), and ferrihydrite ($\text{Fe}(\text{OH})_3$), except for LGO, wherein gypsum had the highest SI. The precipitates from the use of concrete aggregates also followed a different trend, dictated by the metal component rather than the presence of hydroxides and oxyhydroxides.

4.2. Effect of Particle Size on Acid Mine Drainage Treatment

The trend of pH shown in Figure 8a for this batch experiment was based from the amount of material exposed to the AMD in contrast to the jar test which is significantly affected by the amount of alkalinity generating component from each neutralizing agent. The trend was consistent with the size ranges being tested as the highest pH was obtained from the small particle size, which is attributed to the total surface area exposed and reacted with the AMD. However, only minute differences between the obtained pH was observed from each particle size range which may be accounted to the minor size differences concrete aggregate; thus, a more significant variation of sizes may be employed in order to further understand their effects.

As for the removal of Fe, majority was removed using the smallest particle size which attained a pH value of 6.78. Its successful removal can be attributed to its supposed precipitation at a pH range of 3.0–6.0 and would dissolve again at pH 7.0 and above. Since the pH of the AMD had almost reached a value of 7.0, it would suggest that this may have caused the leftover dissolved Fe concentration of around 180 ppm. On the other hand, Al removal is more efficient with larger particles. This may be due to the rate of pH change in the treated AMD. The longer neutralization time needed by larger particles may benefit the formation of Al precipitates, which translates to a higher Al removal from AMD. This trend is also observed for sulfates which may be highly influenced by the speciation of Al

over time and similarly affected by the rate of pH change. However, the limited data available from the experiment need to be expanded to verify this claim.

5. Conclusions

This study was conducted to determine the AMD treatment efficiency of low-grade nickel ore, limestone, fly ash, and concrete aggregates as alternative alkaline-generating materials at varying AMD/Media ratio following a 1-h contact time. After which, the effect of particle size was evaluated using the material that displayed the most significant result from the first batch of experiment. The optimal AMD/Media ratio was used for the second batch of experiment while maintaining the residence time to 1 h and varying grain size from 4.75 mm to 2.00 mm.

Results from the first batch of experiment showed that concrete aggregate provided the most significant result among the four neutralizing agents that were used. Although fly ash was able to elevate the pH of AMD to 9.34, AMD treated with concrete aggregates displayed the most improvement based on geochemical properties and heavy metal concentrations. Alternatively, despite a high percentage removal of sulfate (82.22%) obtained using LGO, the treated AMD had a pH of 4.66 which is very far from the acceptable pH range of 6.5–9.0. Limestone, on the other hand, had the least percentage removal of sulfates (32.47%) despite it having a significant percentage removal for heavy metals. It was also not able to neutralize the AMD to at least neutral level.

The second batch of experiment showed that the smallest particle size range of concrete aggregates had the best performance in neutralizing AMD at the optimal pH of 6.78. The differences in pH for each size range were recorded at minimal values due to the minute difference between the size ranges used. Consequently, it is recommended for future studies to use varying particle sizes with significant size differences. In addition to expanding the difference in particle size, methods that can employ mechanical mixing during the treatment can be developed to improve the neutralizing capability of concrete aggregates.

Author Contributions: Conceptualization, A.H.O. and A.B.B.; methodology, A.H.O. and C.O.A.T.; validation, C.O.A.T., A.H.O. and R.D.A.; writing—original draft preparation, G.B.S. and B.T.M.; writing—review and editing, C.O.A.T. and A.H.O.; visualization, G.B.S. and B.T.M.; supervision, A.H.O.; project administration, A.H.O.; and funding acquisition, A.H.O. All authors have read and agreed to the published version of the manuscript.

Funding: This research was funded by the Department of Science and Technology—Philippine Council for Industry, Energy, and Emerging Technology Research and Development (DOST-PCIEERD), Project No. 04660.

Acknowledgments: The researchers would like to acknowledge Agata Mining Ventures Inc. (AMVI, Agusan Del Norte, Philippines) for their support in the procurement of materials used in this research, and Hirofumi Hinode of Tokyo Institute of Technology for his assistance in the XRF and XRD analysis of the low-grade nickel ore and limestone samples.

Conflicts of Interest: The authors declare no conflict of interest.

References

1. Igarashi, T.; Herrera, P.; Uchiyama, H.; Miyamae, H.; Iyatomi, N.; Hashimoto, K.; Tabelin, C. The two-step neutralization ferrite-formation process for sustainable acid mine drainage treatment: Removal of copper, zinc and arsenic, and the influence of coexisting ions on ferritization. *Sci. Total Environ.* **2020**, *715*, 136877. [[CrossRef](#)] [[PubMed](#)]
2. Skousen, J.; Ziemkiewicz, P.; McDonald, L. Acid mine drainage formation, control and treatment: Approaches and strategies. *Extr. Ind. Soc.* **2019**, *6*, 241–249. [[CrossRef](#)]
3. Tabelin, C.; Igarashi, T.; Villacorte-Tabelin, M.; Park, I.; Opiso, E.; Ito, M.; Hiroyoshi, N. Arsenic, selenium, boron, lead, cadmium, copper, and zinc in naturally contaminated rocks: A review of their sources, modes of enrichment, mechanisms of release, and mitigation strategies. *Sci. Total Environ.* **2018**, *645*, 1522–1553. [[CrossRef](#)] [[PubMed](#)]
4. Simate, G.S.; Ndlovu, S. Acid mine drainage: Challenges and opportunities. *J. Environ. Chem. Eng.* **2014**, *2*, 1785–1803. [[CrossRef](#)]

5. Berk, B.; Pemmasani, N.; Phagura, S. Acid Mine Drainage Treatment Public Policy Report. 2015. Available online: <https://www.cmu.edu/epp/people/faculty/course-reports/NTCReport2015-AcidMineDrainage.pdf> (accessed on 7 September 2020).
6. Park, I.; Tabelin, C.; Jeon, S.; Li, X.; Seno, K.; Ito, M.; Hiroyoshi, N. A review of recent strategies for acid mine drainage prevention and mine tailings recycling. *Chemosphere* **2019**, *219*, 588–606. [CrossRef]
7. Quintans, J. Mining industry in the Philippines. *The Manila Times*. 2017. Available online: <https://www.manilatimes.net/2017/09/04/supplements/mining-industry-philippines/348610/#:~:text=THE%20Philippines%20is%20the%20fifth,mineral%20wealth%2C%20as%20of%202012> (accessed on 7 September 2020).
8. Mines & Geosciences Bureau. Mining Industry Statistics. 2020. Available online: https://mgb.gov.ph/images/Mineral_Statistics/MIS_Q12020_May292020.pdf (accessed on 7 September 2020).
9. Kefeni, K.; Msagati, T.; Mamba, B. Acid mine drainage: Prevention, treatment options, and resource recovery: A review. *J. Clean. Prod.* **2017**. [CrossRef]
10. Huyen, D.; Tabelin, C.; Thuan, H.; Dang, D.; Truong, P.; Vonghuthone, B.; Kobayashi, M.; Igarashi, T. The solid-phase partitioning of arsenic in unconsolidated sediments of the Mekong Delta, Vietnam and its modes of release under various conditions. *Chemosphere* **2019**, *233*, 512–523. [CrossRef]
11. Akcil, A.; Koldas, S. Acid mine drainage (AMD): Causes, treatment and case studies. *J. Clean. Prod.* **2006**, *14*, 1139–1145. [CrossRef]
12. Li, X.; Gao, M.; Hiroyoshi, N.; Tabelin, C.; Taketsugu, T.; Ito, M. Suppression of pyrite oxidation by ferric-catecholate complexes: An electrochemical study. *Miner. Eng.* **2019**, *138*, 226–237. [CrossRef]
13. Pierre Louis, A.; Yu, H.; Shumlas, S.; Van Aken, B.; Schoonen, M.; Strongin, D. Effect of Phospholipid on Pyrite Oxidation and Microbial Communities under Simulated Acid Mine Drainage (AMD) Conditions. *Environ. Sci. Technol.* **2015**, *49*, 7701–7708. [CrossRef]
14. Holmes, P.; Crundwell, F. The kinetics of the oxidation of pyrite by ferric ions and dissolved oxygen: An electrochemical study. *Geochim. Cosmochim. Acta* **2000**, *64*, 263–274. [CrossRef]
15. Chen, M.; Lu, G.; Guo, C.; Yang, C.; Wu, J.; Huang, W.; Yee, N.; Dang, Z. Sulfate migration in a river affected by acid mine drainage from the Dabaoshan mining area, South China. *Chemosphere* **2015**, *119*, 734–743. [CrossRef] [PubMed]
16. Skousen, J.G.; Sextone, A.; Ziemkiewicz, P. Acid mine drainage control and treatment. *Reclam. Drastically Disturb. Lands* **2000**. [CrossRef]
17. Waters, J.C.; Santomartino, S. Acid rock drainage treatment technologies: Identifying appropriate solutions. In Proceedings of the 6th International Conference on Acid Rock Drainage, Cairns, QLD, Australia, 14–17 July 2003.
18. Skousen, J.; Ziemkiewicz, P. Performance of 116 passive treatment systems for acid mine drainage. In Proceedings of the 2005 National Meeting of the American Society of Mining and Reclamation, Breckenridge, CO, USA, 19–23 June 2005. [CrossRef]
19. Morallo, A. DENR to Close 21 Mining Firms. *The Philippine Star*. 2017. Available online: <https://www.philstar.com/business/2017/02/02/1668370/denr-close-21-mining-firms> (accessed on 31 May 2020).
20. Masindi, V.; Akinwekomi, V. Comparison of mine water neutralisation efficiencies of different alkaline generating agents. *J. Environ. Chem. Eng.* **2017**, *5*, 3903–3913. [CrossRef]
21. Potgieter-Vermaak, S.S.; Potgieter, J.H. Comparison of limestone, dolomite and fly ash as pre-treatment agents for acid mine drainage. *Miner. Eng.* **2005**, *19*, 454–462. [CrossRef]
22. Ziemkiewicz, P.F.; Skousen, J.G.; Lovett, R. Open limestone channels for treating acid mine drainage: A new look at an old idea. *Green Lands* **1994**, *24*, 36–41.
23. Cravotta, C.A., III; Trahan, M.K. Limestone drains to increase pH and remove dissolved metals from acidic mine drainage. *Appl. Geochem.* **1999**, *14*, 581–606. [CrossRef]
24. Arnold, D.E. Diversion wells—A low-cost approach to treatment of acid mine drainage. In Proceedings of the Twelfth West Virginia Surface Mine Drainage Task Force Symposium, Morgantown, WV, USA, 3–4 April 1991.
25. Hedin, R.; Narin, R.; Kleinmann, R. *The Passive Treatment of Coal Mine Drainage*; Bureau of Mines IC 9389; U.S. Department of the Interior: Washington, DC, USA, 1994.
26. Muliwa, A.; Leswifi, T. Performance evaluation of eggshell waste material for remediation of acid mine drainage from coal dump leachate. *Miner. Eng.* **2018**, *122*, 241–250. [CrossRef]

27. Heviánková, S.; Bestová, I. The application of wood ash as a reagent in acid mine drainage treatment. *Miner. Eng.* **2014**, *56*, 109–111. [[CrossRef](#)]
28. Ouakibi, O.; Hakkou, R. Phosphate carbonated wastes used as drains for acidic mine drainage passive treatment. *Procedia Eng.* **2014**, *83*, 407–414. [[CrossRef](#)]
29. Kamal, N.M.; Sulaiman, S.K. Bench-Scale study of acid mine drainage treatment using local neutralisation agents. *Malays. J. Fundam. Appl. Sci.* **2014**, *10*, 150–153. [[CrossRef](#)]
30. Cowan, C.E.; Zachara, J.M.; Resch, C.T. Cadmium adsorption on iron oxides in the presence of alkaline-earth elements. *Environ. Sci. Technol.* **1991**, *25*, 437–446. [[CrossRef](#)]
31. The Editors of Encyclopaedia Britannica. 2017. Carbonate Mineral. Available online: <https://www.britannica.com/science/carbonate-mineral> (accessed on 23 June 2020).
32. Bernier, L.R. The potential use of serpentinite in the passive treatment of acid mine drainage: Batch experiments. *Environ. Geol.* **2005**, *47*, 670–684. [[CrossRef](#)]
33. Turingan, C.; Singson, G.; Melchor, B.; Alorro, R.; Beltran, A.; Orbecido, A. A comparison of acid mine drainage (AMD) neutralization potential of low grade nickel laterite and other alkaline-generating materials. *J. Mater. Sci. Chem. Eng.* **2020**. [[CrossRef](#)]
34. Benjamin, M.M.; Leckie, J.O. Multiple-Site adsorption of Cd, Cu, Zn, and Pb on amorphous iron oxyhydroxide. *J. Colloid Interface Sci.* **1981**, *79*, 209–221. [[CrossRef](#)]
35. Balistrieri, L.S.; Chao, T. Adsorption of selenium by amorphous iron oxyhydroxide and manganese dioxide. *Geochim. Cosmochim. Acta* **1990**, *54*, 739–751. [[CrossRef](#)]
36. Zachara, J.M.; Girvin, D.C.; Schmidt, R.L.; Resch, C.T. Chromate adsorption on amorphous iron oxyhydroxide in the presence of major groundwater ions. *Environm. Sci. Technol.* **1987**, *21*, 589–594. [[CrossRef](#)]
37. Holcim, G.T.Z. Reuse and Recycling of Construction and Demolition Waste. 2007. Available online: <https://pdfs.semanticscholar.org/5963/263e9892bc081f55928f45fe9ff09eaa51bb.pdf> (accessed on 4 September 2020).
38. Kalaw, M.; Culaba, A.; Hinode, H.; Kurniawan, W.; Gallardo, S.; Promentilla, M. Optimizing and Characterizing Geopolymers from Ternary Blend of Philippine Coal Fly Ash, Coal Bottom Ash and Rice Hull Ash. *Materials* **2016**, *9*, 580. [[CrossRef](#)]
39. Parkhurst, D.L.; Appelo, C.A.J. Description and Input and Examples for PHREEQC Version 3—A Computer Program for Speciation, Batch-Reaction, One-Dimensional Transport, and Inverse Geochemical Calculations. In *USGS Techniques and Methods 6-A43*; USGS: Denver, CO, USA, 2013.
40. Jones, S.; Cetin, B. Evaluation of waste materials for acid mine drainage remediation. *Fuel* **2017**, *188*, 294–309. [[CrossRef](#)]
41. Parisatto, M.; Dalconi, M.; Valentini, L.; Artioli, G.; Rack, A.; Tucoulou, R.; Cruciani, G.; Ferrari, G. Examining microstructural evolution of Portland cements by in-situ synchrotron micro-tomography. *J. Mater. Sci.* **2014**, *50*, 1805–1817. [[CrossRef](#)]
42. Habeeb, G.; Mahmud, H. Study on Properties of Rice Husk Ash and Its Use as Cement Replacement Material. *Mater. Res.* **2010**, *13*. [[CrossRef](#)]
43. Henmi, T.; Wells, N. Poorly-Ordered iron-rich precipitates from springs and streams on andesitic volcanoes. *Geochim. Cosmochim. Acta* **1980**, *44*, 365–372. [[CrossRef](#)]
44. Jambor, J.L.; Dutrizac, J.E. Occurrence and constitution of natural and synthetic ferrihydrite, a widespread iron oxyhydroxide. *Chem. Rev.* **1998**, *98*, 2549–2586. [[CrossRef](#)] [[PubMed](#)]
45. Koeppenkastrop, D.; De Carlo, E.H. Sorption of rare-earth elements from seawater onto synthetic mineral particles: An experimental approach. *Chem. Geol.* **1992**, *95*, 251–263. [[CrossRef](#)]
46. Soler, J.M.; Boi, M. The passivation of calcite by acid mine water: Column experiments with ferric sulfate and ferric chloride solutions at pH 2. *Appl. Geochem.* **2008**, *23*, 3579–3588. [[CrossRef](#)]
47. Offeddu, F.; Cama, J. Processes affecting the efficiency of limestone in passive treatments for AMD: Column experiments. *J. Environ. Chem. Eng.* **2015**, *3*, 304–316. [[CrossRef](#)]
48. Ya, Z.; Zhou, L. High efficiency of heavy metal removal in mine water by limestone. *Chin. J. Geochem.* **2009**, *28*, 293–298. [[CrossRef](#)]
49. The Editors of Encyclopaedia Britannica. Hydroxide. Britannica. 2017. Available online: <https://www.britannica.com/science/hydroxide> (accessed on 31 May 2020).
50. Liu, H.; Chen, T. An overview of the role of goethite surfaces in the environment. *Chemosphere* **2014**, *103*, 1–11. [[CrossRef](#)]

51. Rietra, R.P.; Hiemstra, T. Sulfate adsorption on goethite. *J. Colloid Interface Sci.* **1999**, *218*, 511–521. [[CrossRef](#)]
52. Cornell, R.M.; Schwertmann, U. *The Iron Oxides: Structure, Properties, Reactions, Occurrence and Uses*; VCH: Weinheim, Germany, 2003; Volume 2, p. 15.
53. Ma, M.; Gao, H.; Sun, Y.; Huang, M. The adsorption and desorption of Ni(II) on Al substituted goethite. *J. Mol. Liq.* **2015**, *201*, 30–35. [[CrossRef](#)]
54. Silva, R.; Cadornin, L.; Rubio, J. Sulphate ions removal from an aqueous solution: I. Co-precipitation with hydrolysed aluminum-bearing salts. *Miner. Eng.* **2010**, *23*, 1220–1226. [[CrossRef](#)]
55. Skousen, J.; Politan, K. Acid mine drainage treatment systems: Chemicals and costs. *Green Lands* **1990**, *20*, 31–37.
56. Miller, A.; Figueroa, L.; Wildeman, T. Zinc and nickel removal in simulated limestone treatment of mining influenced water. *Appl. Geochem.* **2011**, *26*, 125–132. [[CrossRef](#)]
57. Vadapalli, V.; Klink, M.; Etchebers, O.; Petrik, L.; Gitari, W.; White, R.; Key, D.; Iwuoha, E. Neutralization of Acid Mine Drainage using Fly Ash and Strength Development of the Resulting Solid Residues. *South Afr. J. Sci.* **2008**, *104*, 317–322.
58. Golab, A.; Peterson, M.; Indraratna, B. Selection of potential reactive materials for a permeable reactive barrier for remediating acidic groundwater in acid sulphate soil terrains. *Fac. Eng. Pap.* **2006**, *39*. [[CrossRef](#)]



© 2020 by the authors. Licensee MDPI, Basel, Switzerland. This article is an open access article distributed under the terms and conditions of the Creative Commons Attribution (CC BY) license (<http://creativecommons.org/licenses/by/4.0/>).